Published in final edited form as:
Dev Biol. 2011 October 1; 358(1): 79–90. doi:10.1016/j.ydbio.2011.07.020.

Kruppel-like factor 5 is Required for Formation and Differentiation of the Bladder Urothelium

Sheila. M. Bell[1], **Liqian Zhang**[1], **Angela Mendell**[2], **Yan Xu**[1], **Hans Michael Haitchi**[1,Ψ], **James L. Lessard**[2], and **Jeffrey A. Whitsett**[1,*]

[1]Perinatal Institute of Cincinnati Children's Hospital Medical Center, Divisions of Neonatology-Perinatal-Pulmonary Biology, University of Cincinnati College of Medicine. 3333 Burnet Avenue Cincinnati, OH 45229

[2]Developmental Biology, University of Cincinnati College of Medicine. 3333 Burnet Avenue Cincinnati, OH 45229

SUMMARY

Kruppel-like transcription factor 5 (*Klf5*) was detected in the developing and mature murine bladder urothelium. Herein we report a critical role of KLF5 in the formation and terminal differentiation of the urothelium. The Shh^{GfpCre} transgene was used to delete the $Klf5^{floxed}$ alleles from bladder epithelial cells causing prenatal hydronephrosis, hydroureter, and vesicoureteric reflux. The bladder urothelium failed to stratify and did not express terminal differentiation markers characteristic of basal, intermediate, and umbrella cells including keratins 20, 14, and 5, and the uroplakins. The effects of *Klf5* deletion were unique to the developing bladder epithelium since maturation of the epithelium comprising the bladder neck and urethra were unaffected by the lack of KLF5. mRNA analysis identified reductions in *Pparγ, Grhl3, Elf3,* and *Ovol1*expression in *Klf5* deficient fetal bladders supporting their participation in a transcriptional network regulating bladder urothelial differentiation. KLF5 regulated expression of the *mGrhl3* promoter in transient transfection assays. The absence of urothelial *Klf5* altered epithelial-mesenchymal signaling leading to the formation of an ectopic alpha smooth muscle actin positive layer of cells subjacent to the epithelium and a thinner detrusor muscle that was not attributable to disruption of SHH signaling, a known mediator of detrusor morphogenesis. Deletion of *Klf5* from the developing bladder urothelium blocked epithelial cell differentiation, impaired bladder morphogenesis and function causing hydroureter and hydronephrosis at birth.

Keywords

bladder; vesicoureteral reflux; KLF5; GRHL3; urothelium; micro-CT

*Corresponding author: Dr. Jeffrey Whitsett Cincinnati Children's Hospital Medical Center Division of Pulmonary Biology MLC 7029 3333 Burnet Avenue Cincinnati, OH 45229 USA Phone: 1- 513-803-2790 Fax: 1-513-636-7868 Jeffrey.Whitsett@cchmc.org.
ΨPermanent address: Division of Infection, Inflammation, and Immunity, School of Medicine, University of Southampton & Welcome Trust Clinical Research Facility & Respiratory Biomedical Research Unit, Southampton University Hospital Trust, UK.

INTRODUCTION

Congenital disorders of the kidney and urinary tract include renal dysplasia, hydroureter, vesicoureteric reflux (VUR), and bladder outlet obstruction (Kerecuk et al., 2008). VUR involves the retrograde flow of urine from the bladder to the kidneys, placing affected individuals at risk for upper urinary tract infections leading to renal scarring and ultimately renal failure. VUR presents in 1-2% of all children and ~8% of patients with VUR develop end-stage renal failure (Murer et al., 2007; Kerecuk et al., 2008). The embryological origin of VUR has been attributed to several different mechanisms. In humans and mice, *Pax2* heterozygosity delays the disassociation of the ureter from the Wolffian duct resulting in a shortened intravesicle ureter with an aberrant angle of entry into the bladder causing VUR (Murawski et al., 2007). Incorrectly positioned distal ureters resulting in ureteric obstruction, hydronephrosis, and megaureters are observed in *Rar α β* double mutants and *Ret*-/- animals (Mendelsohn et al., 1994; Srinivas et al., 1999). In contrast, over expression of *Ret* results in malformed kidneys and VUR (Yu et al., 2004). VUR also occurs in humans and mice with duplicate ureters due to inappropriate positioning of the ureters into the bladder wall (Murer et al., 2007; Murawski and Gupta, 2008). A delay in the timing of ureteric bud outgrowth and distal ureter contact with the UGS is observed in mice in the absence of *Lim1* resulting in VUR, renal hypoplasia, and dilated ureters (Pedersen et al., 2005). Animals deficient in either uroplakin 3a (*Upk3a*) or *UpkII* exhibit VUR and hydronephrosis indicating that a lack of normal cytoskeletal organization within urothelial cells can contribute to VUR (Hu et al., 2000; Kong et al., 2004).

Although derived from different embryological lineages, the epithelium lining in both the ureters and bladder differentiates into a stratified urothelium with well defined morphological and cellular characteristics. The mature urothelium consists of three distinct cell layers: basal, intermediate and superficial. Cell proliferation is highest in the basal cell layer and is sometimes observed in the intermediate cells (Ayres et al., 1985). The superficial cells, also termed umbrella cells, are highly adapted to maintain a permeability barrier between urine and blood. The surface area of the urothelium changes dynamically with the cycles of contraction and distension of the bladder as it empties and fills. These functions involve a unique apical membrane specialization of the umbrella cells that produces an asymmetrical unit membrane comprised of integral membrane proteins belonging to the uroplakin (*Upk*) gene family (Wu et al., 2009). With the exception of *Upk3b*, *Upk*s are expressed exclusively in urothelial cells during advanced stages of differentiation. The paracellular barrier of the urothelium is mediated by differential expression of tight junction proteins including the claudins (*Cldn*). The expression and localization of several CLDN family members has been associated with specific urothelial cell types and stages of urothelial maturation (Acharya et al., 2004; Varley et al., 2006). Urothelial maturation also involves alterations in cytokeratin (*Krt*) gene expression (Baskin et al., 1996). The expression of *Krts 5* and *14* is initiated and co-localized with *Krts 7* and *19* in basal and intermediate cells (Smith et al., 2002). Fully differentiated umbrella cells uniquely express *Krt 20* (Erman et al., 2006). Although the morphology and cell types comprising the bladder urothelium are well characterized, little is known of the transcription factors and pathways that mediate urothelial maturation.

Kruppel-like transcription factor 5 (KLF5) is expressed in highly proliferative epithelial cell types during embryogenesis and in the adult including the skin, gut, prostate, lung, mammary gland, and bladder, as well as in immortalized epithelial cell lines and proliferating primary cultures (McConnell et al., 2007). Embryonic stem cell studies indicate an important role for KLF5 in self-renewal and the maintenance of pluripotency (Nandan and Yang, 2009). We previously demonstrated that KLF5 is required for terminal maturation of lung epithelial cells (Wan et al., 2008). In the present study, we demonstrate that KLF5 is

required for normal maturation of the murine bladder urothelium and suggest that *Grhl3* and *Pparγ* are candidate transcriptional downstream targets that mediate this process. Deletion of *Klf5* from the developing bladder urothelium causes prenatal VUR, hydroureter, and hydronephrosis.

MATERIALS AND METHODS

Animals

Animal protocols were approved by the Institutional Animal Care and Use Committee in accordance with NIH guidelines. Animals harboring the Shh^{GfpCre} allele were purchased from Jackson Laboratories (Bar Harbor, ME) and mated with $Klf5^{flox/flox}$ animals. $Klf5^{flox/flox}$ females were time mated to $Klf5^{flox/+}Shh^{GfpCre}$ males overnight and the presence of a vaginal plug defined as embryonic day 0.5 (E0.5). For immunohistochemistry, embryos were fixed in paraformaldehyde (4%) in PBS and subsequently dehydrated in graded ethanols for paraffin embedding or equilibrated in 30% sucrose prior to embedding in OCT. Genomic DNA isolated from fetal tails was used for genotyping.

β-Galactosidase staining—For whole mount visualization, dissected urinary tracts were fixed 2 hours in 2% PFA, 0.25% gluteraldehyde in PBS, rinsed 3 times in PBS, and developed for 8 hours in 5 mM $K_3Fe(CN_6)$, 5 mM $K_4Fe(CN_6)$, 2 mM $MgCl_2$, 0.01% Sodium deoxycholate, 0.2% NP-40, and 1 mg/ml X-Gal. Stained tissues were equilibrated in sucrose and embedded in OCT prior to sectioning.

Micro computerized tomography—E18.5 whole fetuses were fixed and stored in 4% paraformaldehyde in PBS. Forty-eight hours prior to imaging, fetuses were rinsed in PBS and placed in isotonic 25% Iodine solution as described by Degenhardt et al. (2010). Images were obtained using a microCAT II micro CT using a kVp of 80 and an anode current of 225 micro-amps. 776 projections were collected through 194 degrees of gantry rotation using an x-ray exposure time of 2.30 sec and a bin factor of 2. The set of projections was reconstructed using COBRA (cone beam reconstruction algorithm, Exxim Computing Corporation, Pleasanton, CA USA). The reconstructed image voxel size was 19.4 microns isotropic. The raw CT slice data were loaded in to Amira (Visage Imaging, San Diego, CA USA) for viewing and conversion to DICOM format that have been viewed and processed in OsiriX, an open-source image processing software (Pixmeo, Geneva, Switzerland).

Immunohistochemistry—Paraffin embedded tissue was sectioned at 6 μm, dewaxed, rehydrated in graded ethanols, subjected to antigen retrieval (as necessary using 0.1M citrate buffer, pH 6.0, and heat), and endogenous peroxidase activity was quenched in methanol and H_2O_2 for 15 minutes. Frozen sections were cut at 7 μm, dried overnight and fixed in 4% PFA for 10 minutes prior to antigen retrieval and quenching. Primary antibodies requiring antigen retrieval were guinea pig anti-KLF5 (in house, 1:1500; Wan et al., 2008), mouse anti-Keratin14 (Neomarkers LL002, 1:300), rabbit anti-Keratin 5 (in house, 1:1000), rabbit anti-FOXA1 (Seven Hills Bioreagents, 1:1000), rabbit anti-SOX2 (Seven Hills Bioreagents, 1:2500), rabbit anti-SOX9 (Millipore, AB5535, 1:800), rabbit anti-PhosphoHistone H3 (SantaCruz, SC8656R, 1:500), rat anti-Ki67 (Dako, TEC-3 clone M7249, 1:1000), p63 (Santa Cruz, SC71827, 1:500), mouse anti-smoothelin (Millipore, MAB3242, 1:200), chicken anti-Beta Galactosidase (Abcam, ab9361, 1:3000), rat anti-cyclin D1 (Millipore, 04-1151, 1:1000) and rabbit anti-PAX2 (Invitrogen, 716000, 1:1000). Other antibodies included rabbit anti-Desmin (Abcam, 152001, 1:400), mouse anti-α-smooth muscle actin (Sigma, monoclonal 1A4, 1:6,000); goat anti-UPK1B (Santa Cruz, Ni20, 1:100), and anti-KRT20 (Dako, monoclonal KS20.8 M7019, 1:25). Biotinylated secondary antibodies (1:200, Vector Laboratories) were detected using an avidin-biotin-horseradish-peroxidase

detection system (ABC reagent, Vector Laboratories, Burlingame, CA). Sections were counterstained with Nuclear Fast Red. As a negative control, primary antibody was omitted on some slides. At least three animals of each genotype were evaluated at each time point using the antibodies indicated.

Real-time RT-qPCR—Total RNA was isolated from E14.5 or E16.5 embryonic bladders dissected free from the ureters and urethra using the QIAGEN microRNA isolation kit. $Klf5^{wt/wt}Shh^{GfpCre+}$ embryos were used for the control sample. cDNA was generated using the Versa RT-kit (ThermoScientific). At least three independent cDNA samples were used per genotype. cDNA samples were amplified in triplicate on a StepOne Plus Real Time PCR system (Applied Biosystems). All values were normalized to ribosomal protein 18s within the sample and values calculated using the $2^{-\Delta\Delta CT}$ (Livak) method. The Applied Biosystems TAQMAN primer pairs used were *Klf5* (Mm00456521_m1), *Pparγ* (Mm01184322_m1), *Grhl3* (Mm01193339_m1), *p63* (Mm00495788_m1), *Ovol1* (Mm00498263_m1), *Elf3* (Mm01295975_m1), *Shh* (Mm00436527_m1), *Ptch1* (Mm00436026_m1), *Gli1* (Mm00494645_m1), *Gli2* (Mm01293116_m1), and *Bmp4* (Mm00432087_m1).

Reflux evaluation—The bladders of E18.5 and P0 mice were surgically exposed following removal of the gastrointestinal tract. $Klf5^{flox/flox}Shh^{GfpCre-}$, $Klf5^{flox/wt}Shh^{GfpCre-}$, and $Klf5^{flox/wt}Shh^{GfpCre+}$ littermates were used as the controls. A 1 cc syringe filled with India ink was attached to a 30-gauge needle. The needle was inserted into the bladder lumen and a small volume of ink was delivered followed by palpation of the external surface of the bladder wall. Each fetus was evaluated for the appearance of ink in the ureters, renal pelvi, and evacuation out the urethra.

Urothelial cell proliferation—Bladders from 4 $Klf5^{\Delta/\Delta}$ and 4 controls (either $Klf5^{+/+}Shh^{GfpCre+}$ or $Klf5^{flox/flox}Shh^{GfpCre-}$) embryos were sectioned. Three sections per E16.5 bladder were taken approximately 100 μM apart and stained for phospho-Histone H3 (pHH3). The entire luminal surface of each bladder section (except the region containing and distal to the trigone) was photographed using a 20X objective. The total number of pHH3 positive cells and the total number of urothelial cells were determined using MetaMorph software (Molecular Devices; Sunnyvale, CA). For each embryo, the number of pHH3 positive nuclei and total nuclei were summed from the three sections to determine the percentage of pHH3 positive nuclei/bladder. These values were subjected to a 2-tailed paired Student t-test.

mRNA Microarray analysis—Total RNA from E14.5 whole bladders isolated from $Klf5^{\Delta/\Delta}$ and $Klf5^{+/+}Shh^{GfpCre+}$ embryos (n=3 samples/genotype, each sample a pool of two bladders) was isolated using the Qiagen MicroRNA Kit. The cDNA was then hybridized according to the manufacturer's protocol to the Affymetrix Mouse Gene 1.0 ST Array, covering 28,853 genes with approximately 27 probes per gene spread across the full length of each gene. The RNA quality and quantity assessment, probe preparation, labeling, hybridization and image scan were carried out in the CCHMC Affymetrix Core using standard procedures. Hybridization data were sequentially subjected to normalization, transformation, filtration, functional classification and pathway analysis as previously described (Xu et al., 2009). Data analysis was performed with Genespring GX11. All probe sets on the array were pre-filtered based on their signal intensity such that a probe was kept for further analysis if the probe signal intensity was > 35th percentile in at least 2 of 3 samples. Differentially expressed genes in response to *Klf5* deletion vs control mice were identified using an unpaired Student t-test. Changes in gene expression were considered statistically significant if their p value was less than 0.05 and fold-change was greater than 1.5. Gene Ontology Analysis was performed using the publicly available web-based tool

DAVID (database for annotation, visualization, and integrated discovery)(Huang da et al., 2009). A gene ontology term is considered to be overly-represented when a Fisher's exact test P value is ≤ 0.001 and gene hits are ≥ 5. The complete dataset can be accessed from geo@ncbi.nlm.nih.gov by the accession number GSE27014.

Transient transfection assays—The *mGrhl3* promoter was isolated by PCR using the primers 5'-GCATAAAGAAGGCTTGGCACG-3' and 5'GGCTGGAAGCACAGGTGCCGACTG-3' to amplify a 1744 bp product which was sequence verified and subcloned into pGL4 (Promega) to create *GL4mGrhl3Luc*. T24 (human bladder epithelial transitional carcinoma, ATCC HTB-4) and HEK293T (human embryonic kidney epithelia) cells were grown to 40% confluence in six well plates and transfected with plasmid DNA (0.5 μg) using FuGene 6 (Roche). Promoter activity was determined by measurement of luciferase activity normalized to β-galactosidase activity 48 hours after transfection. All experiments were done in triplicate in 3 independent experiments. Lipofectamine 2000 (Invitrogen) was used to transfect 100 pmoles of either *hKlf5* (Am16708) or control (Am4611) siRNA (Ambion). Part of each lysate was utilized for Western Blot analysis. Blots were hybridized with a guinea pig anti-KLF5 antibody (Wan et al., 2008; 1:4000) and rabbit anti-GAPDH (Abcam, ab9485, 1:5000) as a loading control.

RESULTS

Developmental Expression of KLF5 in the Urinary Tract

Immunohistochemical (IHC) analysis revealed that KLF5 was expressed in the invaginating cloacal epithelium beginning on E10.5. At E14.5, E16.5, and E18.5, KLF5 was detected in the epithelium lining the bladder, bladder neck, urethra, ureter and kidney (Fig.1 A-C, data not shown). In the fetal and adult bladder urothelium KLF5 was detected in all cell layers (Fig. 1B'), with the lowest levels of expression in the terminally differentiated umbrella cells.

Deletion of *Klf5* by Shh^{GfpCre}

To begin to understand the role of KLF5 in maturation of the bladder urothelium, $Klf5^{floxed}$ animals were mated with animals harboring the Shh^{GfpCre} allele in which an EGFP*Cre*-recombinase fusion cassette was inserted into the start site of the *Shh* locus resulting in *Cre* expression under control of the endogenous *Shh* promoter (Harfe et al., 2004; Seifert et al., 2008). *Shh* expression begins as early as E10 in the lung and invaginating cloacal epithelium and is expressed throughout the bladder epithelium until at least E14.5 (Harris et al., 2006; Haraguchi et al., 2007). KLF5 IHC revealed an almost complete loss of KLF5 in the bladder, bladder neck, and urethral epithelium of the urinary tract, as well as the lung epithelium of E14.5 (n=3), E16.5 (n=5), and E18.5 (n=6) $Klf5^{flox/flox}Shh^{GfpCre+}$ ($Klf5^{\Delta/\Delta}$) fetuses (Fig. 1D-F, data not shown). Consistent with our previous studies deleting *Klf5* using lung specific drivers, all $Klf5^{\Delta/\Delta}$ fetuses died shortly after birth of respiratory distress (Wan et al., 2008). Previous reports indicated that *Shh* is expressed in the developing ureter and kidney (Yu et al., 2002). KLF5 expression was maintained in the ureter and renal pelvis $Klf5^{\Delta/\Delta}$ mice (Fig. 1E, 2H, data not shown). Shh^{GfpCre} dependent recombination at the *Rosa26* locus was evaluated by whole mount β-galactosidase staining of dissected urogenital tracts and/or IHC for β-galactosidase. Both analyses indicated inefficient levels of recombination within the ureters with the highest levels of recombination present in the most proximal third of the ureters (Fig. 1 G-H). Little to no recombination occurred in the middle and distal regions of the ureters (Fig. 1G, I). Combined these observations indicate that *Klf5* is not efficiently removed from the ureteric epithelium by the Shh^{GfpCre} allele.

Hydroureter, hydronephrosis, and VUR after deletion of *Klf5*

At E18.5 and P0, the ureters and renal pelvi of all $Klf5^{\Delta/\Delta}$ fetuses were dilated. Hydroureter and hydronephrosis were confirmed by visualization, serial sectioning, and high resolution micro-computerized tomography (CT)(Fig. 2). Differences in size or structure of the kidneys at E14.5 and E16.5 were not detected by IHC staining for PAX2 or SOX9 (Fig. 2E,F, data not shown). Injection of India ink into the bladder lumen followed by palpation of the bladder resulted in vesicoureteric reflux in 6/6 $Klf5^{\Delta/\Delta}$ fetuses that occurred bilaterally in 4 of the 6 fetuses (Fig. 2A vs B). In contrast, of the 10 nonmutants evaluated, only 1 exhibited reflux and it was unilateral. In previous studies, VUR was attributed to defects in formation of the kidneys and/or ureters (Chang et al., 2004; Airik et al., 2006, 2010; Iizuka-Kogo et al., 2007; Murawski et al., 2007; Nie et al., 2010). In all $Klf5^{\Delta/\Delta}$ fetuses a single ureter and kidney were observed bilaterally, indicating that VUR is not attributable to duplications of the kidneys and/or ureters.

Deletion of *Klf5* from the bladder epithelium prohibits stratification and differentiation of the urothelium

The *ShhCre* transgene was highly active in the bladder urothelium resulting in efficient early deletion of *Klf5* that inhibited maturation of the bladder urothelium. At E14.5, a single cell layered epithelium lined the forming bladder in $Klf5^{\Delta/\Delta}$ embryos, whereas epithelial stratification was evident in control embryos (Fig. 1A,D). As urothelial maturation proceeded, three distinct cell layers: basal, intermediate, and umbrella were first evident in control fetuses at E16.5 (Fig. 1B') and persisted at E18.5. As seen at E14.5, a single cell layered epithelium lined the bladder of E16.5 and E18.5 $Klf5^{\Delta/\Delta}$ fetuses (Fig 1D-F). At E16.5, p63 expression was predominantly localized to basal cells in control mice and was dramatically reduced or undetectable (Fig. 3A,A' vs B,B') in the single layer of cells lining the bladder of $Klf5^{\Delta/\Delta}$ fetuses. Unlike p63, expression of FOXA1 persisted in most cells comprising the single layered epithelium lining the E16.5 and E18.5 $Klf5^{\Delta/\Delta}$ bladders while in control mice a gradient of FOXA1 expression was established with the highest levels of expression present in the terminally differentiated umbrella cell layer (Fig. 3C,C',D,D'). At E18.5, umbrella cells within the superficial layer of control fetuses expressed KRT20 and UPK1B (Fig. 4A,C). KRT14 and KRT5 were expressed in the basal and intermediate cell layers of the bladder urothelium (Fig. 4E, data not shown). UPK1B, KRT20, KRT14 or KRT5 were not detected in the simple epithelium lining the bladder of $Klf5^{\Delta/\Delta}$ fetuses indicating the absence of terminally differentiated basal and umbrella cells (Fig. 4B,D,F, data not shown).

In contrast, stratification of the urothelium of control and $Klf5^{\Delta/\Delta}$ ureters was initiated by E16.5 (Fig. 2E, F inserts) although fewer cell layers were noted in $Klf5^{\Delta/\Delta}$ fetuses. At E18.5, KLF5 was detected in most cells lining the ureteric epithelium of $Klf5^{\Delta/\Delta}$ fetuses (Fig. 2H). However, the urothelium of control fetuses possessed 2-3 cell layers whereas only 1-2 cell layers were evident in the dilated ureters of $Klf5^{\Delta/\Delta}$ fetuses Fig. 2G, H). Whether this difference in appearance is attributable to the dilated state of the ureter or partly to incomplete recombination of the $Klf5^{floxed}$ allele within this tissue is not known. Ureters from $Klf5^{\Delta/\Delta}$ E18.5 fetuses expressed UPK1B (Fig. 2K,L) and Keratin 20 (KRT20)(data not shown) indicating that the ureteric urothelium expresses mature urothelial markers. Alpha smooth muscle actin (αSMA) was detected in smooth muscle surrounding the dilated renal pelvi and proximal ureters of $Klf5^{\Delta/\Delta}$ mice (Fig. 2I-J). Taken together these data indicate that in contrast to the profound affect on morphogenesis of the bladder urothelium, the ureteric urothelium undergoes normal terminal differentiation suggesting that the observed hydroureters are not attributable to deficiencies in ureter urothelial maturation.

Normal maturation of *Klf5* deficient bladder neck and urethral epithelium

The bladder, bladder neck, and urethral epithelium are all derived from the cloacal epithelium (Seifert et al., 2008). In sharp contrast to the findings in the bladder, the absence of KLF5 in the bladder neck and urethra did not prohibit their normal differentiation. In the normal bladder, bladder neck and urethral epithelium; KLF5, p63, FOXA1, KRT14 and KRT5 were expressed by cells within all three compartments, whereas expression of the uroplakins was restricted to the bladder urothelium (Figs. 1C, 3A-A", 3C-C", 4E, data not shown)(Romih et al., 2005). Distinction between the epithelium destined to form the bladder versus the bladder neck/urethra was demarcated by E14.5 in both control and $Klf5^{\Delta/\Delta}$ embryos by regionalized expression of SOX2 (Fig. 3G,H). Normal expression of p63, FOXA1, KRT14, KRT5, and cyclin D1 was observed in the bladder neck and urethral epithelium of $Klf5^{\Delta/\Delta}$ fetuses Fig. 3B, 3B", 3D, 3D", 3F, 4F, and data not shown). These observations reveal a critical role of KLF5 in formation and differentiation of the bladder urothelium but not the adjacent bladder neck and urethral epithelium.

Deletion of *Klf5* does not alter urothelial proliferation at E14.5 or E16.5

Phosphohistone H3 (pHH3) and Ki67 stains were similar in control and $Klf5^{\Delta/\Delta}$ mice at E14.5 and E16.5. At E16.5 the proliferative rate was quantified by determining the percentage of phosphohistone H3 positive cells within the epithelial population of the bladder lumen in control and $Klf5^{\Delta/\Delta}$ fetuses. A statistically significant difference was not observed between cellular proliferation in KLF5 deficient (24.07 ± 4.76 s.e.m.) and control (28.02 ± 4.61 s.e.m.)($p = 0.572$) bladder epithelium. In TSU-Pr1 human bladder cancer cells and other tissues, KLF5 induced cellular proliferation by activating cyclin D1 expression (Sun et al., 2001; Nandan et al., 2005; Chen et al., 2006; Yang et al., 2007; Ema et al., 2008). Cyclin D1 staining was absent in the maturing bladder urothelium at E14.5, E15.5 and E16.5 in both control and $Klf5^{\Delta/\Delta}$ bladder epithelium (Fig. 3E-F, and data not shown). A few cells stained positively for cyclin D1 in the bladder epithelium of controls and $Klf5^{\Delta/\Delta}$ fetuses at E18.5. In contrast, cyclin D1 was detected in basal cells of the bladder neck at E16.5 and E18.5 in both control and *Klf5* deficient epithelium. Due to the absence of effects on epithelial cellular proliferation in the $Klf5^{\Delta/\Delta}$ bladder epithelium, we evaluated cell death. Tunnel assay detected few dying cells in E16.5 control or $Klf5^{\Delta/\Delta}$ epithelia (data not shown). Combined these data indicate that cellular proliferation within the bladder epithelium and bladder neck are not altered by the absence of KLF5 and suggest that within the bladder neck epithelium cyclin D1 expression is not dependent upon KLF5.

Inhibition of Urothelial Maturation After Deletion of *Klf5*

mRNA microarray analysis was performed on cDNA from whole bladder total RNA isolated from E14.5 $Klf5^{\Delta/\Delta}$ and $Klf5^{wt/wt}Shh^{Gfp\text{-}Cre+}$ embryos. Of the 363 genes differentially expressed ≥ 1.5 fold with a $p \leq .05$, GO analysis identified two major subgroupings, epithelial cell development/differentiation (GO:007398, GO:0030855, GO: 0060429 GO:0008544) and cell adhesion (GO:0016337 and GO:0022610). As early as E14.5, $Klf5^{\Delta/\Delta}$ tissue expressed reduced levels of urothelial terminal differentiation markers including Upk1a, Upk1b, Upk3a, Ivl, Sprr1a, Sprr2a, Krt8, Krt4, Krt18, Krt7, Cldn8, Cldn4, Cldn7, and *Emp1* (Table I) (Smith et al., 2002; Acharya et al., 2004; Erman et al., 2006; Wu et al., 2009). These observations are consistent with our previous developmental profiling of the urothelium that indicated that expression of many terminal differentiation markers was initiated as early as E13.5 (www.GUDMAP.org). As indicated in Table 1, a number of genes previously identified as KLF5 targets following over expression in ES cells were oppositely affected by deletion of *Klf5* in maturing bladder epithelial cells.

KLF5 deficiency alters the expression of transcription factors associated with urothelial maturation

Decreased expression of only 11 transcription factors was observed after deletion of *Klf5*: *Ehf* (-3.46, p<.0044), *Pparγ* (-3.33, p<.0011), *Elf3* (-2.85, p<.00026), *Grhl3* (-2.56, p< . 0018), *Msx2* (-2.2 p<.0003), *Foxq1* (-2.19, p<.0041), *Foxa1* (-1.85, p<.022), *Zfp750* (-1.77, p<.00067), *Ovol1* (-1.62, p<.00082), *Elf5* (-1.6, p<.031), and *Tcfap2c* (-1.53, p<.0099). Three of these genes were previously implicated in urothelial terminal differentiation: *Pparγ* (peroxisome proliferator-activated receptor γ), *Grhl3* (grainyhead-like 3) and *FoxA1* (Varley et al., 2009; Yu et al., 2009). Quantitative real-time PCR of E14.5 whole bladder cDNA confirmed reductions in *Klf5, Pparγ, Grhl3, Elf3*, and *Ovol1* expression (Fig. 5A). Although p63 staining was decreased at E16.5, p63 mRNA levels were not altered at E14.5. Taken together, deletion of *Klf5* in the bladder urothelium arrested urothelial maturation as early as E14.5.

KLF5 regulation of *Grhl3* in vitro

Since the defect observed in urothelial maturation in $Grhl3^{-/-}$ fetuses was less severe than that observed in the $Klf5^{\Delta/\Delta}$ embryos, we postulated that *Grhl3* is a downstream target of KLF5 (Yu et al., 2009). We created the reporter construct *GL4mGrhl3Luc* containing 1.7 kb of the mouse *Grhl3* promoter driving luciferase gene expression. MatInspector analysis of the *mGrhl3* promoter identified 8 putative KLF binding sites located between -1250 and -1 (Cartharius et al., 2005). *GL4mGrhl3Luc* was active in T24 bladder and HEK293T cells (Fig. 5B, C). Co-transfection of the *Klf5* expression construct, *pKlf5*, induced *GL4mGrhl3Luc* activity in HEK293T cells while cotransfection into T24 cells did not potentiate activity of the *mGrhl3* promoter, perhaps related to the high levels of endogenous KLF5 in these cells. Co-transfection of *Klf5* siRNA into T24 cells reduced *GL4mGrhl3Luc* activity (p≤ .00467) that was accompanied by a reduction in the levels of KLF5 (Fig. 5D). The decrease in *Grhl3* mRNA seen in $Klf5^{\Delta/\Delta}$ bladders in vivo coupled with these in vitro data support the concept that *Grhl3* is a downstream target of KLF5.

Deletion of *Klf5* influences bladder smooth muscle formation

The profound effect of *Klf5* deficiency on maturation of the urothelium was accompanied by alterations in development of the surrounding mesenchyme that forms the smooth muscle and stromal layers of the bladder. The musculature of the bladder wall was frequently thinner in $Klf5^{\Delta/\Delta}$ fetuses compared to controls (Figs. 1C vs F, 3C vs D, 4E vs F, 6A-D). A prominent layer of cells was seen in all E18.5 $Klf5^{\Delta/\Delta}$ fetuses that stained positively for αSMA and desmin subjacent to the luminal epithelium that was absent or represented by a few cells in the controls ($Klf5^{flox/flox}Shh^{GfpCre-}$ and $Klf5^{flox/+}Shh^{GfpCre+}$)(Fig. 6A vs B, data not shown). The ectopic αSMA positive layer of cells was first detected at E16.5 in the bladder dome of $Klf5^{\Delta/\Delta}$ fetuses. Smoothelin staining was only detected in the detrusor muscle of control and $Klf5^{\Delta/\Delta}$ E18.5 fetuses, indicating that the ectopic αSMA staining population of cells was not likely mature smooth muscle (Fig. 6C vs D).

Maturation of the bladder musculature is influenced by SHH signaling from the epithelium to the subjacent mesenchyme (Tasian et al., 2010). At E14.5 no alterations in the expression of αSMA, serum response factor, *Shh*, or any of the SHH downstream targets *Ptch1, Gli1, Gli2*, or *Bmp4* implicated in formation of the detrusor were detected in the mRNA microarray analysis or by RT-qPCR of E14.5 and E16.5 whole bladders. At both developmental time points, the levels of expression of the components of the SHH signaling pathway were highly variable in both control and $Klf5^{\Delta/\Delta}$ tissues consistent with the dynamic regulation of SHH signaling during this window of development (Fig. 6E) (Tasian et al., 2010). Such variability was not seen in the same samples when RT-qPCR was performed in the transcription factor analysis (Fig. 5A, data not shown). These observations indicate that

formation of the ectopic α-SMA positive cell layer is not likely attributable to alterations in known components of the SHH signaling pathway and is perhaps dependent on the alteration of other urothelium derived signals.

DISCUSSION

Klf5 deficiency in the developing bladder urothelium provides a unique model of congenital functional obstructive uropathy presenting with the prenatal occurrence of VUR, hydroureter, and hydronephrosis. In contrast to other mouse models, hydroureter and hydronephrosis seen after deletion of *Klf5* were related to epithelial differentiation or morphogenetic abnormalities in the bladder rather than to physical obstruction, altered peristalsis or defects in ureteric budding resulting in VUR due to inappropriate positioning of the ureters into the bladder wall (Chang et al., 2004; Airik et al., 2006, 2010; Iizuka-Kogo et al., 2007; Murawski et al., 2007; Nie et al., 2010). Since *Klf5* expression was maintained in the developing kidney and ureter in the present model, we propose that VUR, hydroureters, and hydronephrosis are likely secondary consequences of bladder dysmorphogenesis. Serial sectioning of $Klf5^{\Delta\Delta}$ E18.5 fetuses indicated that the bladders of many fetuses were distended and the smooth muscle layer was thin when compared to controls. These findings are similar to those in the human syndromes megacystis-microcolon-intestinal hypoperistalsis (OMIM 249210) and Eagle-Barrett (Denes et al., 2004) also characterized by bladder distention, hydroureters, and hydronephrosis at birth but for which genetic causes have not been identified. Megacystis followed by hydroureter and hydronephrosis is also observed in the *Megabladder (Mgb)* mouse (Singh et al., 2007; Ingraham et al., 2010). Although the gene responsible for the *Mgb* phenotype has not been identified, the urothelium is normal and the primary defect is thought to be intrinsic to the maturing smooth muscle progenitor cells of the developing bladder. A known regulator of bladder smooth muscle maturation is SHH signaling from the epithelium to the underlying mesenchyme (Tasian et al., 2010). $Shh^{-/-}$ and $Gli2^{-/-}$ fetuses exhibit bladder hypoplasia (Haraguchi et al., 2007). Like $Klf5^{\Delta/\Delta}$ fetuses, $Gli2^{-/-}$ fetuses also possess an ectopic αSMA positive cell layer subjacent to the bladder epithelium whose formation was attributed to a reduction in *Bmp4* expression by the mesenchyme (Cheng et al., 2008). Our examination of *Shh*, *Ptc1*, *Gli2*, *Gli1* and *Bmp4* mRNAs indicated that SHH signaling from the urothelium to the PTC1 receptor in the mesenchyme was likely not altered in the $Klf5^{\Delta/\Delta}$ bladder, suggesting that other KLF5-dependent signals made by the maturing urothelium mediate normal radial patterning of the bladder mesenchyme. Prior studies in rats, demonstrated that at postnatal day 10 an α-SMA, desmin, vimentin, and vinculin positive cell layer was first detected subjacent to the urothelium (Baskin et al., 1996). In the adult human bladder, suburothelial cells that express α-SMA, desmin, and vimentin but not smoothelin are referred to as muscularis mucosa (Council and Hameed, 2009). In humans and guinea pigs the suburothelial cells termed myofibroblasts/intersitial cells of the bladder are characterized by their expression of α-SMA, desmin, vimentin, c-kit, and Cx43 and are currently thought to relay signals from the urothelium to the detrusor (Drake et al., 2006; Fry et al., 2007; McCloskey, 2010). In the present study, the absence of staining for smoothelin in the suburothelial region suggests that the α-SMA positive layer of cells observed in $Klf5^{\Delta/\Delta}$ fetuses at E18.5 may represent precocious formation of the interstitial cells of the lamina propria that may contribute to fetal bladder dysfunction in the present model.

Abnormalities in urothelial maturation have been reported in only a few mouse models. *Upk3a* and *UpkII* are expressed exclusively by urothelial cells during advanced stages of differentiation. The ureteric urothelium becomes thickened leading to occlusion and VUR in adult mice lacking the uroplakins (Hu et al., 2000; Kong et al., 2004). Formation of a multilayered urothelium is dependent on FGF7 signaling from the mesenchyme to the overlying epithelium (Tash et al., 2001). The intermediate cell layer is absent and basal and

umbrella cells are intermixed within the single cell layered urothelium of *Fgf7*$^{-/-}$ mice; in contrast to the single layered epithelium observed in *Klf5*$^{\Delta/\Delta}$ fetuses that lacked terminally differentiated basal and umbrella cells. The mRNA microarray analysis of E14.5 *Klf5*-deficient bladders did not detect alterations in expression of *Fgf7* or its receptor, *Fgfr2* (Finch et al., 1995). In the absence of *p63* a single urothelial cell layer expressing *Upks* forms. Although *p63* is expressed by basal cells that give rise to the intermediate and umbrella cells, *p63* expression is not a prerequisite for maturation of umbrella-like cells (Signoretti et al., 2005; Cheng et al., 2006). Therefore, the lack of p63 in *Klf5*$^{\Delta/\Delta}$ urothelium does not explain the failure of terminal differentiation. The absence of p63, KRT5, and KRT14 expression in the single layer of cells lining the *Klf5*$^{\Delta/\Delta}$ bladder suggests these cells are not basal cells. The persistent uniform expression of FOXA1, and the lack of expression of terminal differentiation markers of basal, intermediate, and umbrella cells indicates that in the absence of KLF5, urothelial precursor cells remain in an undifferentiated state.

Little is known of the transcriptional hierarchy regulating urothelial maturation. *Pparγ, Grhl3, Ovol1, Foxa1, Elf3* and *Ehf* are coordinately expressed with *Klf5* in the developing bladder and other embryonic epithelial tissues (http//:genepaint.org) (Auden et al., 2006; Feldman et al., 2003; Li et al., 2006; Oettgen et al., 1997). We have determined that KLF5 regulates transcription of the *Grhl3* gene in vitro. Although several putative “KLF” binding sites were identified by MatInspector analysis (Cartharius et al., 2005), three distinct KLF5 consensus binding sites were recently proposed based on genes commonly identified in samples subjected to CHIP Seq and mRNA Microarray analysis (Parisi et al., 2010). An examination of 1.7 kb of the *mGrhl3* promoter with these sequences identified 7 putative KLF5 binding sites. Thus *Grhl3* may be a direct downstream target of KLF5 during urothelial maturation. Consistent with this concept, *Grhl3*$^{-/-}$ fetuses form a stratified urothelium with a defect in formation of the terminally differentiated umbrella cells (Yu et al., 2009). Transglutaminase I (*Tgm1*), a key enzyme in epithelial barrier formation, and *UpkII* are direct downstream targets of GRHL3 (Ting et al., 2005; Yu et al., 2009). In addition to *Tgm1* and *UpkII*, previous studies indicated that the expression of *Sprr1a, Snx31, Fmo5, Tmprss13,* and *Adh1* normally increase during the course of bladder maturation. The expression of all of these genes was down regulated in both E14.5 *Klf5*$^{\Delta/\Delta}$ and in E18.5 *Grhl3*$^{-/-}$ bladders (Table I)(Yu et al., 2009).

Several lines of evidence also suggest that *Pparγ* plays a critical role in regulating urothelial maturation. *Pparγ* expression increases as the mouse urothelium matures (Jain et al., 1998) and PPARγ activation by the agonist troglitazone induced expression of the terminal differentiation markers, *Upks la, 1b, II* and *IIIa, Krt13, Krt20* and *Cldn3* in cultured human urothelial cells (Varley et al., 2004; Varley et al., 2006; Varley et al., 2009). In committed urothelial cells, PPARγ induced *FoxA1* and *Irf1* that directly interacted with cis –regulatory elements in the *Upk1a, 2,* and *3a* gene promoters (Varley et al., 2009). In the differentiated E18.5 urothelium, FOXA1 was expressed at the highest levels in the umbrella cell layer suggesting that this signaling paradigm occurs during initial maturation of the mouse urothelium. By E14.5, a dramatic reduction in *Pparγ* expression occurred in *Klf5*$^{\Delta/\Delta}$ bladders accompanied by greater reductions in the expression of *Upk1a, 2,* and *3a* and the absence of terminally differentiated urothelial cells. KLF5 directly regulates *Pparγ* expression during the differentiation of adipocytes (Oishi et al., 2005). The present observations suggest that KLF5 may also regulate *Pparγ* during the process of urothelial maturation.

Developmental roles for *Elf3* and *Ovol1* in maturation of the bladder have not been previously proposed. Prior studies of *Elf3* deficient mice revealed that ELF3 is required for normal development of the intestinal epithelium (Ng et al., 2002), morphogenesis of the urothelium was not evaluated. *Elf3* expression was dramatically increased in adult urothelium in response to infection and has been shown to directly regulate claudin 7

expression (Mysorekar et al., 2002), Kohno et al., 2006). In the dermis, *Ovol1* is required for committed epidermal progenitor cells to exit from proliferation (Nair et al., 2006). *Ovol1*-deficient mice are unable to properly form the skin barrier and develop cystic kidneys (Teng et al., 2007). A Kruppel-like binding site was previously identified at position -167 within the *mOvol1* promoter (Li et al., 2002). Further study of the regulatory mechanisms controlling the expression of these genes will provide new insights into the urothelial differentiation program and provide new paradigms for understanding differentiation and perhaps repair in other epithelial tissues.

Several lines of evidence have suggested that cyclin D1 is regulated by KLF5 (Bateman et al., 2004; Nandan et al., 2004, 2005). Cyclin D1 was increased in bladder cancer cells over expressing KLF5 that showed an increase in the rate of proliferation (Chen et al., 2006). In the present study, changes in the proliferation rate in the bladder urothelium were not noted between controls and $Klf5^{\Delta/\Delta}$ mice. We also observed that between E14.5 and E16.5, cyclin D1 protein was not detectable in the normal urothelium indicating that proliferation is not dependent on KLF5 or cyclin D1 during this period of development. In contrast to the bladder urothelium, epithelial cells within the fetal bladder neck were proliferative and expressed cyclin D1 even in the absence of KLF5. KLF5 deficient embryonic stem cells (ESC) exhibit a decreased rate of cellular proliferation associated with altered regulation of the cyclin-dependent kinase inhibitor, *p21*, and the Akt co-activator *Tcl1* (Ema et al., 2008). Alterations in these genes were also not observed in the microarray analysis of mRNA isolated from E14.5 whole bladders. In ESC, KLF5 deficiency can be compensated for by KLF2 and KLF4 (Ema et al., 2008; Jiang et al., 2008; Nandan and Yang, 2009). Compensation by KLF2 or KLF4 is unlikely in the $Klf5^{\Delta/\Delta}$ bladder epithelium since *Klf4* mRNA expression was restricted to the bladder mesenchyme and *Klf2* expression was not detectable (http://www.genepaint.org).

The present findings support the concept that activities of KLF5 are highly dependent on developmental context, being critical for embryonic urothelial maturation rather than maintenance of proliferation. These studies demonstrate a novel role for KLF5 as a critical regulator of urothelial maturation during late embryonic development. We propose that *Pparγ* and *Grhl3* may participate in a KLF5 dependent gene network regulating maturation of the urothelium.

Acknowledgments

This work was funded in part by NIH R01:HL-090156 (J.A.W.). The authors would like to thank Gail Macke for technical assistance and Dr. Ron Pratt from the Imaging Research Center at Cincinnati Children's Hospital for obtaining and reconstructing the original Micro CT scan images. H.M.H. is a visiting scholar at the University of Cincinnati College of Medicine and a clinician funded by the Medical Research Council, London, UK.

REFERENCES

Acharya P, Beckel J, Ruiz WG, Wang E, Rojas R, Birder L, Apodaca G. Distribution of the tight junction proteins ZO-1, occludin, and claudin-4, -8, and -12 in bladder epithelium. Am J Physiol Renal Physiol. 2004; 287:F305–18. [PubMed: 15068973]

Airik R, Bussen M, Singh MK, Petry M, Kispert A. Tbx18 regulates the development of the ureteral mesenchyme. J Clin Invest. 2006; 116:663–74. [PubMed: 16511601]

Airik R, Trowe MO, Foik A, Farin HF, Petry M, Schuster-Gossler K, Schweizer M, Scherer G, Kist R, Kispert A. Hydroureternephrosis due to loss of *Sox9*-regulated smooth muscle cell differentiation of the ureteric mesenchyme. Hum Mol Genet. 2010; 19:4918–29. [PubMed: 20881014]

Auden A, Caddy J, Wilanowski T, Ting SB, Cunningham JM, Jane SM. Spatial and temporal expression of the Grainyhead-like transcription factor family during murine development. Gene Expr Patterns. 2006; 6:964–70. [PubMed: 16831572]

Ayres PH, Shinohara Y, Frith CH. Morphological observations on the epithelium of the developing urinary bladder of the mouse and rat. J Urol. 1985; 133:506–12. [PubMed: 3974006]

Baskin LS, Hayward SW, Young PF, Cunha GR. Ontogeny of the rat bladder: smooth muscle and eipthelial differentiation. Acta Anat. 1996; 155:163–171. [PubMed: 8870784]

Bateman NW, Tan D, Pestell RG, Black JD, Black AR. Intestinal tumor progression is associated with altered function of KLF5. J Biol Chem. 2004; 279:12093–101. [PubMed: 14726538]

Cartharius K, Frech K, Grote K, Klocke B, Haltmeier M, Klingenhoff A, Frisch M, Bayerlein M, Werner T. MatInspector and beyond: promoter analysis based on transcription factor binding sites. Bioinformatics. 2005; 21:2933–42. [PubMed: 15860560]

Chang CP, McDill BW, Neilson JR, Joist HE, Epstein JA, Crabtree GR, Chen F. Calcineurin is required in urinary tract mesenchyme for the development of the pyeloureteral peristaltic machinery. J Clin Invest. 2004; 113:1051–8. [PubMed: 15057312]

Chen C, Benjamin MS, Sun X, Otto KB, Guo P, Dong XY, Bao Y, Zhou Z, Cheng X, Simons JW, Dong JT. KLF5 promotes cell proliferation and tumorigenesis through gene regulation and the TSU-Pr1 human bladder cancer cell line. Int J Cancer. 2006; 118:1346–55. [PubMed: 16184550]

Cheng W, Jacobs WB, Zhang JJ, Moro A, Park JH, Kushida M, Qiu W, Mills AA, Kim PC. DeltaNp63 plays an anti-apoptotic role in ventral bladder development. Development. 2006; 133:4783–92. [PubMed: 17079275]

Cheng W, Yeung CK, Ng YK, Zhang JR, Hui CC, Kim PC. Sonic Hedgehog mediator Gli2 regulates bladder mesenchymal patterning. J Urol. 2008; 180:1543–50. [PubMed: 18710724]

Council L, Hameed O. Differential expression of immunohistochemical markers in bladder smooth muscle and myofibroblasts, and the potential utility of desmin, smoothelin, and vimentin in staging of bladder carcinoma. Mod Pathol. 2009; 22:639–50. [PubMed: 19252475]

Degenhardt K, Wright AC, Horng D, Padmanabhan A, Epstein JA. Rapid 3D phenotyping of cardiovascular development in mouse embryos by micro-CT with iodine staining. Circ Cardiovasc Imaging. 2010; 3:314–22. [PubMed: 20190279]

Denes FT, Arap MA, Giron AM, Silva FA, Arap S. Comprehensive s urgical treatment of prune belly syndrome: 17 years' experience with 32 patients. Urology. 2004; 64:789–93. discussion 793-4. [PubMed: 15491721]

Drake MJ, Fry CH, Eyden B. Structural characterization of myofibroblasts in the bladder. BJU Int. 2006; 97:29–32. [PubMed: 16336323]

Ema M, Mori D, Niwa H, Hasegawa Y, Yamanaka Y, Hitoshi S, Mimura J, Kawabe Y, Hosoya T, Morita M, Shimosato D, Uchida K, Suzuki N, Yanagisawa J, Sogawa K, Rossant J, Yamamoto M, Takahashi S, Fujii-Kuriyama Y. Kruppel-like factor 5 is essential for blastocyst development and the normal self-renewal of mouse ESCs. Cell Stem Cell. 2008; 3:555–67. [PubMed: 18983969]

Erman A, Veranic P, Psenicnik M, Jezernik K. Superficial cell differentiation during embryonic and postnatal development of mouse urothelium. Tissue Cell. 2006; 38:293–301. [PubMed: 16973199]

Feldman RJ, Sementchenko VI, Watson DK. The epithelial-specific Ets factors occupy a unique position in defining epithelial proliferation, differentiation and carcinogenesis. Anticancer Res. 2003; 23:2125–31. [PubMed: 12894586]

Finch PW, Cunha GR, Rubin JS, Wong J, Ron D. Pattern of keratinocyte growth factor and keratinocyte growth factor receptor expression during mouse fetal development suggests a role in mediating morphogenetic mesenchymal-epithelial interactions. Dev Dyn. 1995; 203:223–40. [PubMed: 7655084]

Fry CH, Sui GP, Kanai AJ, Wu C. The function of suburothelial myofibroblasts in the bladder. Neurourol Urodyn. 2007; 26:914–9. [PubMed: 17763395]

Haraguchi R, Motoyama J, Sasaki H, Satoh Y, Miyagawa S, Nakagata N, Moon A, Yamada G. Molecular analysis of coordinated bladder and urogenital organ formation by Hedgehog signaling. Development. 2007; 134:525–33. [PubMed: 17202190]

Harfe BD, Scherz PJ, Nissim S, Tian H, McMahon AP, Tabin CJ. Evidence for an expansion-based temporal Shh gradient in specifying vertebrate digit identities. Cell. 2004; 118:517–528. [PubMed: 15315763]

Harris KS, Zhang Z, McManus MT, Harfe BD, Sun X. Dicer function is essential for lung epithelium morphogenesis. Proc Natl Acad Sci U S A. 2006; 103:2208–13. [PubMed: 16452165]

Hu P, Deng FM, Liang FX, Hu CM, Auerbach AB, Shapiro E, Wu XR, Kachar B, Sun TT. Ablation of uroplakin III gene results in small urothelial plaques, urothelial leakage, and vesicoureteral reflux. J Cell Biol. 2000; 151:961–72. [PubMed: 11085999]

Huang da W, Sherman BT, Lempicki RA. Systematic and integrative analysis of large gene lists using DAVID bioinformatics resources. Nat Protoc. 2009; 4:44–57. [PubMed: 19131956]

Iizuka-Kogo A, Ishidao T, Akiyama T, Senda T. Abnormal development of urogenital organs in Dlgh1-deficient mice. Development. 2007; 134:1799–807. [PubMed: 17435047]

Ingraham SE, Saha M, Carpenter AR, Robinson M, Ismail I, Singh S, Hains D, Robinson ML, Hirselj DA, Koff SA, Bates CM, McHugh KM. Pathogenesis of Renal Injury in the Megabladder Mouse: A Genetic Model of Congenital Obstructive Nephropathy. Pediatr Res. 2010; 68:500–507. [PubMed: 20736884]

Jain S, Pulikuri S, Zhu Y, Qi C, Kanwar YS, Yeldandi AV, Rao MS, Reddy JK. Differential expression of the peroxisome proliferator-activated receptor gamma (PPARgamma) and its coactivators steroid receptor coactivator-1 and PPAR-binding protein PBP in the brown fat, urinary bladder, colon, and breast of the mouse. Am J Pathol. 1998; 153:349–54. [PubMed: 9708794]

Jiang J, Chan YS, Loh YH, Cai J, Tong GQ, Lim CA, Robson P, Zhong S, Ng HH. A core Klf circuitry regulates self-renewal of embryonic stem cells. Nat Cell Biol. 2008; 10:353–60. [PubMed: 18264089]

Kerecuk L, Schreuder MF, Woolf AS. Renal tract malformations: perspectives for nephrologists. Nat Clin Pract Nephrol. 2008; 4:312–25. [PubMed: 18446149]

Kohno Y, Okamoto T, Ishibe T, Nagayama S, Shima Y, Nishijo K, Shibata KR, Fukiage K, Otsuka S, Uejima D, Araki N, Naka N, Nakashima Y, Aoyama T, Nakayama T, Nakamura T, Toguchida J. Expression of claudin7 is tightly associated with epithelial structures in synovial sarcomas and regulated by an Ets family transcription factor, ELF3. J Biol Chem. 2006; 281:38941–50. [PubMed: 17060315]

Kong XT, Deng FM, Hu P, Liang FX, Zhou G, Auerbach AB, Genieser N, Nelson PK, Robbins ES, Shapiro E, Kachar B, Sun TT. Roles of uroplakins in plaque formation, umbrella cell enlargement, and urinary tract diseases. J Cell Biol. 2004; 167:1195–204. [PubMed: 15611339]

Li B, Mackay DR, Dai Q, Li TW, Nair M, Fallahi M, Schonbaum CP, Fantes J, Mahowald AP, Waterman ML, Fuchs E, Dai X. The LEF1/beta -catenin complex activates movo1, a mouse homolog of Drosophila ovo required for epidermal appendage differentiation. Proc Natl Acad Sci U S A. 2002; 99:6064–9. [PubMed: 11983900]

Li J, Shiroyanagi Y, Lin G, Haqq C, Lin CS, Lue TF, Willingham E, Baskin LS. Serum response factor, its cofactors, and epithelial-mesenchymal signaling in urinary bladder smooth muscle formation. Differentiation. 2006; 74:30–9. [PubMed: 16466398]

McCloskey KD. Interstitial cells in the urinary bladder--localization and function. Neurourol Urodyn. 2010; 29:82–7. [PubMed: 20025023]

McConnell BB, Ghaleb AM, Nandan MO, Yang VW. The diverse functions of Kruppel-like factors 4 and 5 in epithelial biology and pathobiology. BioEssays. 2007; 29:549–57. [PubMed: 17508399]

Mendelsohn C, Lohnes D, Decimo D, Lufkin T, LeMeur M, Chambon P, Mark M. Function of the retinoic acid receptors (RARs) during development (II). Multiple abnormalities at various stages of organogenesis in RAR double mutants. Development. 1994; 120:2749–71. [PubMed: 7607068]

Murawski IJ, Myburgh DB, Favor J, Gupta IR. Vesico-ureteric reflux and urinary tract development in the Pax2 1Neu+/- mouse. Am J Physiol Renal Physiol. 2007; 293:F1736–45. [PubMed: 17881463]

Murawski IJ, Gupta IR. Gene discovery and vesicoureteric reflux. Pediatr Nephrol. 2008; 23:1021–7. [PubMed: 18253765]

Murer L, Benetti E, Artifoni L. Embryology and genetics of primary vesicoureteric reflux and associated renal dysplasia. Pediatr Nephrol. 2007; 22:788–97. [PubMed: 17216254]

Mysorekar IU, Mulvey MA, Hultgren SJ, Gordon JI. Molecular regulation of urothelial renewal and host defenses during infection with uropathogenic Escherichia coli. J Biol Chem. 2002; 277:7412–9. [PubMed: 11744708]

Nair M, Teng A, Bilanchone V, Agrawal A, Li B, Dai X. Ovol1 regulates the growth arrest of embryonic epidermal progenitor cells and represses c-myc transcription. J Cell Biol. 2006; 173:253–64. [PubMed: 16636146]

Nandan MO, Yoon HS, Zhao W, Ouko LA, Chanchevalap S, Yang VW. Kruppel-like factor 5 mediates the transforming activity of oncogenic H Ras. Oncogene. 2004; 23:3404–13. [PubMed: 15077182]

Nandan MO, Chanchevalap S, Dalton WB, Yang VW. Kruppel-like factor 5 promotes mitosis by activating the cyclin B1/Cdc2 complex during oncogenic Ras-mediated transformation. FEBS Lett. 2005; 579:4757–62. [PubMed: 16102754]

Nandan MO, Yang VW. The role of Kruppel-like factors in the reprogramming of somatic cells to induced pluripotent stem cells. Histol Histopathol. 2009; 24:1343–55. [PubMed: 19688699]

Ng AY, Waring P, Ristevski S, Wang C, Wilson T, Pritchard M, Hertzog P, Kola I. Inactivation of the transcription factor *Elf3* in mice results in dysmorphogenesis and altered differentiation of intestinal epithelium. Gastroenterology. 2002; 122:1455–66. [PubMed: 11984530]

Nie X, Sun J, Gordon RE, Cai CL, Xu PX. SIX1 acts synergistically with TBX18 in mediating ureteral smooth muscle formation. Development. 2010; 137:755–65. [PubMed: 20110314]

Oettgen P, Alani RM, Barcinski MA, Brown L, Akbarali Y, Boltax J, Kunsch C, Munger K, Libermann TA. Isolation and characterization of a novel epithelium-specific transcription factor, ESE-1, a member of the ets family. Mol Cell Biol. 1997; 17:4419–33. [PubMed: 9234700]

Oishi Y, Manabe I, Tobe K, Tsushima K, Shindo T, Fujiu K, Nishimura G, Maemura K, Yamauchi T, Kubota N, Suzuki R, Kitamura T, Akira S, Kadowaki T, Nagai R. Kruppel-like transcription factor KLF5 is a key regulator of adipocyte differentiation. Cell Metab. 2005; 1:27–39. [PubMed: 16054042]

Parisi S, Cozzuto L, Tarantino C, Passaro F, Ciriello S, Aloia L, Antonini D, De Simone V, Pastore L, Russo T. Direct targets of Klf5 transcription factor contribute to the maintenance of mouse embryonic stem cell undifferentiated state. BMC Biol. 2010; 8:128. [PubMed: 20875108]

Pedersen A, Skjong C, Shawlot W. Lim 1 is required for nephric duct extension and ureteric bud morphogenesis. Dev Biol. 2005; 288:571–81. [PubMed: 16216236]

Romih R, Korosec P, de Mello W Jr. Jezernik K. Differentiation of epithelial cells in the urinary tract. Cell Tissue Res. 2005; 320:259–68. [PubMed: 15778856]

Seifert AW, Harfe BD, Cohn MJ. Cell lineage analysis demonstrates an endodermal origin of the distual urethra and perineum. Developmental Biology. 2008; 318:143–152. [PubMed: 18439576]

Signoretti S, Pires MM, Lindauer M, Horner JW, Grisanzio C, Dhar S, Majumder P, McKeon F, Kantoff PW, Sellers WR, Loda M. p63 regulates commitment to the prostate cell lineage. Proc Natl Acad Sci U S A. 2005; 102:11355–60. [PubMed: 16051706]

Singh S, Robinson M, Nahi F, Coley B, Robinson ML, Bates CM, Kornacker K, McHugh KM. Identification of a unique transgenic mouse line that develops megabladder, obstructive uropathy, and renal dysfunction. J Am Soc Nephrol. 2007; 18:461–71. [PubMed: 17202422]

Smith FJ, Porter RM, Corden LD, Lunny DP, Lane EB, McLean WH. Cloning of human, murine, and marsupial keratin 7 and a survey of K7 expression in the mouse. Biochem Biophys Res Commun. 2002; 297:818–27. [PubMed: 12359226]

Srinivas S, Wu Z, Chen CM, D'Agati V, Costantini F. Dominant effects of RET receptor misexpression and ligand-independent RET signaling on ureteric bud development. Development. 1999; 126:1375–86. [PubMed: 10068631]

Sun R, Chen X, Yang VW. Intestinal-enriched Kruppel-like factor (Kruppel-like factor 5) is a positive regulator of cellular proliferation. J Biol Chem. 2001; 276:6897–900. [PubMed: 11152667]

Tash JA, David SG, Vaughan EE, Herzlinger DA. Fibroblast growth factor-7 regulates stratification of the bladder urothelium. J Urol. 2001; 166:2536–41. [PubMed: 11696824]

Tasian G, Cunha G, Baskin L. Smooth muscle differentiation and patterning in the urinary bladder. Differentiation. 2010; 80:106–117. [PubMed: 20541860]

Teng A, Nair M, Wells J, Segre JA, Dai X. Strain-dependent perinatal lethality of *Ovol1*-deficient mice and identification of *Ovol2* as a downstream target of Ovol1 in skin epidermis. Biochim Biophys Acta. 2007; 1772:89–95. [PubMed: 17049212]

Ting SB, Caddy J, Hislop N, Wilanowski T, Auden A, Zhao LL, Ellis S, Kaur P, Uchida Y, Holleran WM, Elias PM, Cunningham JM, Jane SM. A homolog of Drosophila grainy head is essential for epidermal integrity in mice. Science. 2005; 308:411–3. [PubMed: 15831758]

Varley CL, Stahlschmidt J, Lee WC, Holder J, Diggle C, Selby PJ, Trejdosiewicz LK, Southgate J. Role of PPARgamma and EGFR signalling in the urothelial terminal differentiation programme. J Cell Sci. 2004; 117:2029–36. [PubMed: 15054105]

Varley CL, Garthwaite MA, Cross W, Hinley J, Trejdosiewicz LK, Southgate J. PPARgamma-regulated tight junction development during human urothelial cytodifferentiation. J Cell Physiol. 2006; 208:407–17. [PubMed: 16688762]

Varley CL, Bacon EJ, Holder JC, Southgate J. FOXA1 and IRF-1 intermediary transcriptional regulators of PPARgamma-induced urothelial cytodifferentiation. Cell Death Differ. 2009; 16:103–14. [PubMed: 18688264]

Wan H, Luo F, Wert SE, Zhang L, Xu Y, Ikegami M, Maeda Y, Bell SM, Whitsett JA. Kruppel-like factor 5 is required for perinatal lung morphogenesis and function. Development. 2008; 135:2563–72. [PubMed: 18599506]

Wu XR, Kong XP, Pellicer A, Kreibich G, Sun TT. Uroplakins in urothelial biology, function, and disease. Kidney Int. 2009; 75:1153–65. [PubMed: 19340092]

Xu Y, Saegusa C, Schehr A, Grant S, Whitsett JA, Ikegami M. C/EBP{alpha} is required for pulmonary cytoprotection during hyperoxia. Am J Physiol Lung Cell Mol Physiol. 2009; 297:L286–98. [PubMed: 19465518]

Yang Y, Goldstein BG, Nakagawa H, Katz JP. Kruppel-like factor 5 activates MEK/ERK signaling via EGFR in primary squamous epithelial cells. FASEB J. 2007; 21:543–50. [PubMed: 17158781]

Yu J, Carroll TJ, McMahon AP. Sonic hedgehog regulates proliferation and differentiation of mesenchymal cells in the mouse metanephric kidney. Development. 2002; 129:5301–12. [PubMed: 12399320]

Yu OH, Murawski IJ, Myburgh DB, Gupta IR. Overexpression of RET leads to vesicoureteric reflux in mice. Am J Physiol Renal Physiol. 2004; 287:F1123–30. [PubMed: 15328070]

Yu Z, Mannik J, Soto A, Lin KK, Andersen B. The epidermal differentiation-associated Grainyhead gene *Get1*/*Grhl3* also regulates urothelial differentiation. EMBO J. 2009; 28:1890–903. [PubMed: 19494835]

Highlights

KLF5 is required for stratification and terminal differentiation of urothelial cells.

Prenatal defects in maturation of the bladder urothelium can induce hydronephrosis, hydroureter, and vesicoureteral reflux.

KLF5 is not required for maturation and stratification of the bladder neck and urethral epithelium.

Grhl3 and *Pparγ* are candidate downstream targets of KLF5 that mediate urothelial maturation.

KLF5 dependent signals regulate morphogenesis of the bladder mesenchyme.

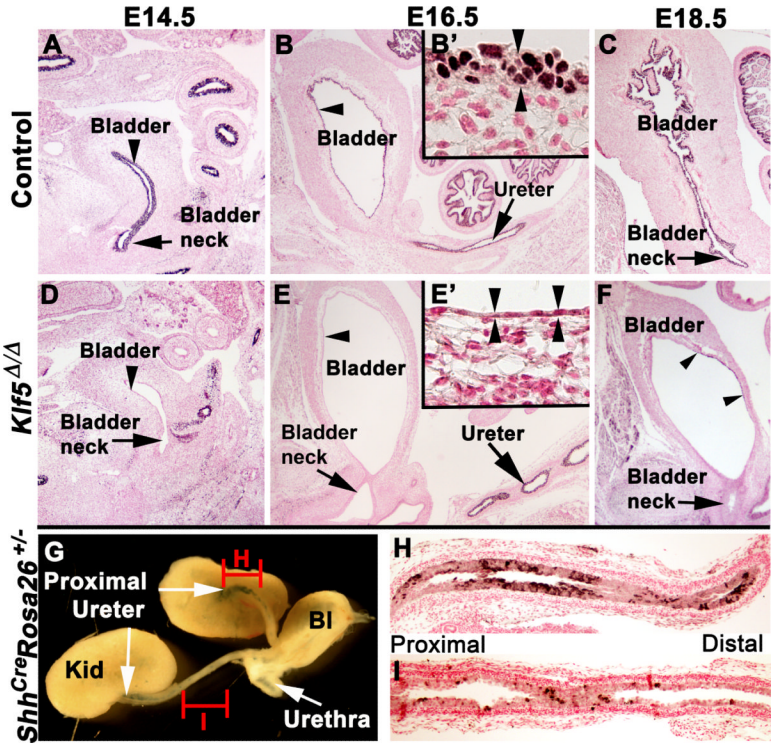

Figure 1. KLF5 expression and efficiency of recombination of the *Klf5*^{floxed} allele by *Shh*^{GfpCre} during bladder and ureter development

KLF5 immunohistochemistry was performed at the indicated embryonic time points. (A-C) control embryos. (D-F) *Klf5*$^{\Delta/\Delta}$ embryos. *Klf5* is efficiently deleted throughout the bladder lumen epithelium (arrowheads) and bladder neck but not from the epithelium of the ureter. B' and E' insets are 10x magnification of the lumen epithelium shown in B and E. Note absence of KLf5 expression and presence of a single cell layer in E' vs 3-4 cells comprise the control (B'). Small region between arrowheads in F shows a segment containing KLF5 positive cells that was observed in the bladders of a few embryos where deletion did not occur. (G) β-galactosidase whole mount staining of an isolated *Shh*^{GfpCre}*Rosa26*$^{+/-}$ urinary tract. Note most staining is restricted to the proximal ureter with little to no staining in the mid and distal ureter. (H-I) IHC staining of sectioned ureters with anti-β-galactosidase. (H) Proximal region indicated in (G) closest to renal pelvis exhibits varying β-galactosidase expression. (I) Within the middle segment of the ureter as indicated in (G) only a few scattered cells express β-galactosidase.

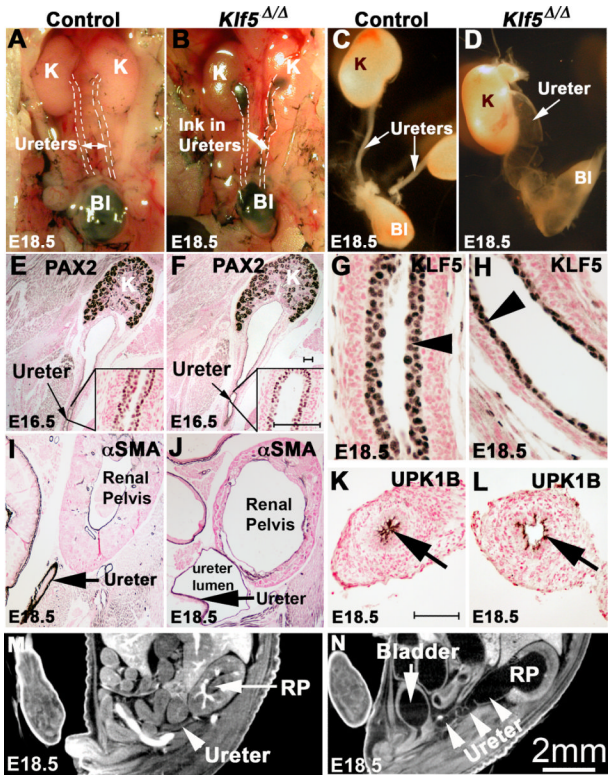

Figure 2. Vesicoureteric reflux, hydroureters, and ureteral maturation in *Klf5*$^{\Delta/\Delta}$ fetuses

(A-B) India ink injection into bladder lumen followed by palpation. (B) Ink is present in ureters and renal pelvi. (C-D) Dissected out urinary tracts. Note hydroureter in D vs C (arrows) and opaqueness of bladder in (D). (E-L) Immunohistochemical staining for the indicated markers. (E-F) Some dilation of the ureter is evident as early as E16.5 in *Klf5*$^{\Delta/\Delta}$ fetuses and the ureteric urothelium appears slightly thinner. Insets are higher magnification of the indicated region. (G-H) The *Klf5*$^{\Delta/\Delta}$ ureteric urothelium expresses KLF5 but is only 1-2 cells thick vs the 2-3 cell layers observed in controls (arrowheads). (I-J) Hydronephrosis and hydroureter in *Klf5* deficient fetuses. Smooth muscle lines the renal pelvis and surrounds the ureter in the *Klf5*$^{\Delta/\Delta}$ fetus and in controls (arrows). (K-L) Ureter cross sections, arrows indicate UPK1B staining on lumenal cells. (A-L) All scale bars represent 10 microns. (M-N) Micro-CT scans of fetuses. (M) Control, (N) *Klf5*$^{\Delta/\Delta}$. A distended bladder, hydronephrosis of the renal pelvis, and a patent hydroureter (arrowheads) are shown. Kidney (K), Bladder (Bl), Renal pelvis (RP).

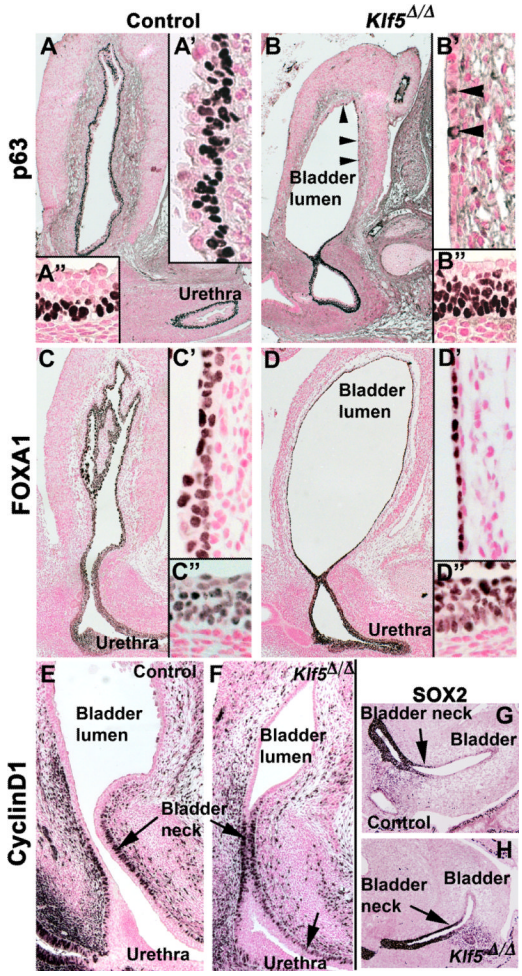

Figure 3. Decreased expression of transcription factors associated with urothelial maturation in the absence of KLF5

(A-F) Immunohistochemical analysis at E16.5 of the indicated proteins. (A'-D') higher magnification of bladder urothelium. (A''-D'') higher magnification of adjacent bladder neck/urethra. The bladder neck/urethra stratified normally in *Klf5*$^{\Delta/\Delta}$ fetuses, whereas the bladder urothelium remained single layered. (E-F) Arrows indicate expression of cyclin D1 within the basal cells of the stratified bladder neck and urethral epithelium. (G-H) E14.5 embryos. Note demarcation in SOX2 positive staining at bottom edge of bladder vs bladder neck region in both control and *Klf5*$^{\Delta/\Delta}$ embryos.

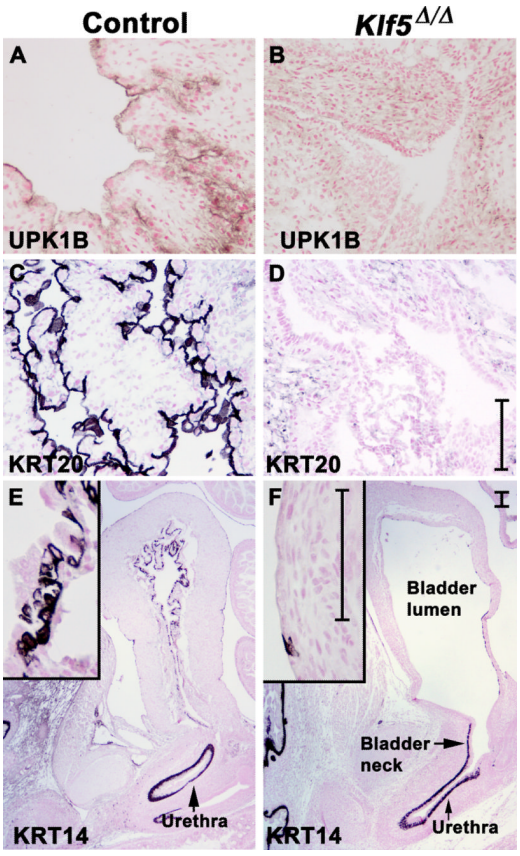

Figure 4. KLF5 is required for maturation of the bladder urothelium

Immunohistochemical staining of control (A,C,E) and *Klf5*$^{\Delta/\Delta}$ (B,D,F) E18.5 fetuses with the antibodies indicated. UPK1B, KRT20, and KRT14 are not expressed by the single layered epithelium lining the *Klf5*$^{\Delta/\Delta}$ bladder. Insets in E and F are higher magnification images of bladder urothelium. Note the normal maturation of bladder neck and urethra that are also *Klf5* deficient. The muscle wall is abnormally thin in the *Klf5*$^{\Delta/\Delta}$ bladder (F). Scale bar in D represents 10 microns for A-D.

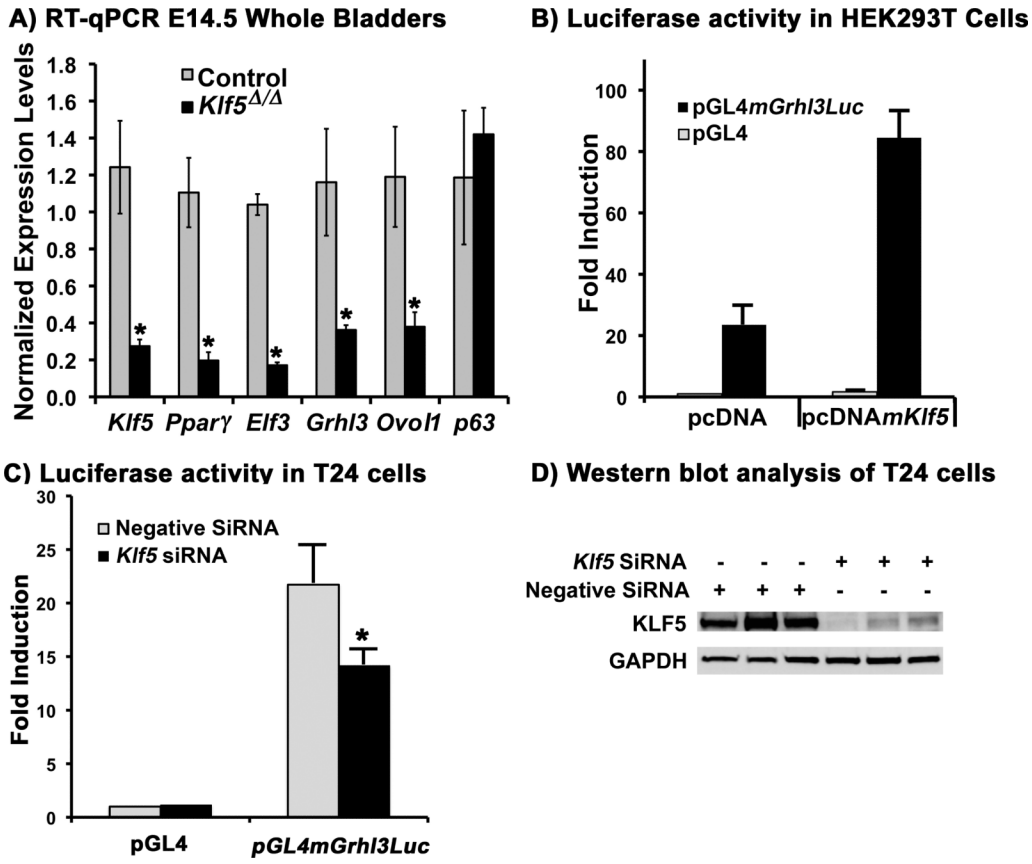

Figure 5. Candidate transcriptional targets of KLF5

(A) Normalized RT-qPCR gene expression of whole bladder cDNAs at E14.5. Asterisks indicate statistically significant differences by Student t-test ($p \leq 0.05$). (B) Regulation of *pGL4mGrhl3Luc* by KLF5 in HEK293T cells. (C) T24 cells transfected with *Klf5* siRNA exhibited diminished *pGL4mGrhl3Luc* activity. (D) Western blot analysis of cell lysates from T24 cells transfected with the indicated SiRNA for the presence of KLF5.

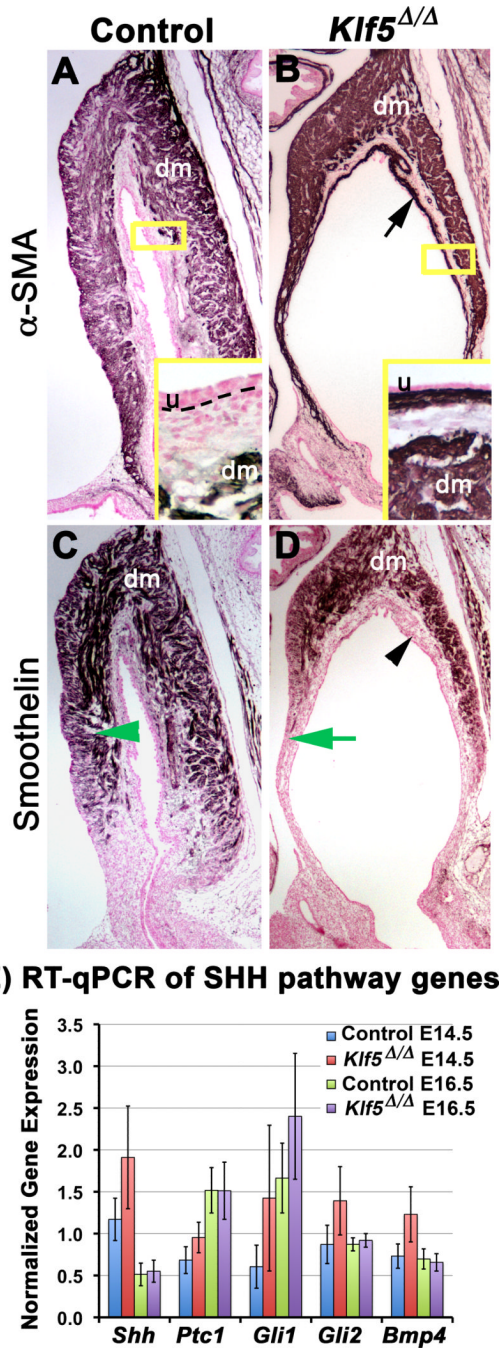

Figure 6. KLF5 is required for normal formation of the bladder mesenchyme

(A-D) Immunohistochemical analysis of E18.5 fetuses for α-smooth muscle actin and smoothelin reveals both markers are expressed by the detrusor muscle (dm). *Klf5*$^{\Delta/\Delta}$ fetuses possess an ectopic α-SMA positive (arrow in B), smoothelin negative (arrowhead in D) region subjacent to the bladder epithelium/urothelium (u) as indicated at higher magnification in insets (A, B). Green arrowhead in (C) indicates thick lateral detrusor muscle compared to diminished bladder wall thickness, green arrowhead in (D). (E) Normalized RT-qPCR gene expression of E14.5 and E16.5 whole bladders suggests SHH signaling is not disrupted in *Klf5*$^{\Delta/\Delta}$ bladders. Bars indicate s.e.m. between individual

samples (E14.5 n=3, E16.5 n=5). No statistically significant differences were observed ($p<.05$).

Table 1

Representative genes differentially regulated in E14.5 *Klf5*$^{\Delta/\Delta}$ bladders compared to controls.

Gene Symbol	Fold Change	P-value	Accession	Effect of *Klf5* over-expression in ES cells[1]
Sprrla	-20.20	0.0004	NM_009264	
Sprr2a	-3.64	0.0004	NM_011468	
Krt4	-3.19	0.0084	NM_008475	
Krt8	-3.38	0.0001	NM_031170	
Krt18	-2.84	0.0003	NM_010664	
Krt15	-2.60	0.0002	NM_008469	
Krt7	-2.81	0.0002	NM_033073	
Upk3A	-3.66	0.0011	NM_023478	
UpklA	-6.44	0.0003	NM_026815	
Upklb	-5.04	0.0002	NM_178924	
Upk2	-8.79	.00004	NM_009476	
Rab27b	-3.60	.00073	NM_001082553	
Ivl	-3.76	0.0006	NM_008412	
Cldn4	-2.13	0.0069	NM_009903	
Tgml	-1.74	0.0009	NM_019984	
Snx31	-5.53	0.0011	NM_025712	
Fmo5	-1.89	0.0023	NM_010232	
Tmprss13	-2.43	0.0001	NM_001013373	
Adh1	-5.846	0.0046	NM_007409	
Klf5	-1.50	0.0073	NM_009769	
Grhl3	-2.56	0.0018	NM_001013756	
Pparγ	-3.33	0.0011	NM_011146	
2310045A20Rik	1.94	0.0313	NM_172710	repressed
Ankrd1	1.65	0.0215	NM_013468	repressed
Ap1m2	-2.02	0.0012	NM_001110300	activated
Emp1	-1.54	0.0121	NM_010128	activated
Foxa1	-1.85	0.0222	NM_008259	repressed
Igfbp7	-1.95	0.0023	NM_008048	repressed
Lamc2	-1.78	0.0050	NM_008485	activated
Lrrn1	2.84	0.0301	NM_008516	repressed
Ntn1	-1.53	0.0202	NM_008744	repressed
Perp	-2.15	0.0002	NM_022032	activated
1600029D21Rik	-6.25	0.0003	NM_029639	activated
AA409316	-2.20	0.0052	NM_134087	activated
Sfn	-2.15	0.0003	XR_034292	activated

[1] As reported in Parisi, S. et al. (2010) BMC Biology 8:128.